UNIVERSITA' DEGLI STUDI DI NAPOLI "FEDERICO II"

University of Naples "Federico II"

DOTTORATO DI RICERCA IN TERAPIE AVANZATE BIOMEDICHE E CHIRURGICHE XXXVI CICLO

PhD Program in Advanced Surgical and Biomedical Therapies - 36° cycle

TESI DI DOTTORATO

PhD Thesis

Artificial Intelligence-assisted Near-INfrared FluorEscence Angiography with Indocyanine green after colorectal resections: The NINFEA study

CANDIDATO
PhD Candidate
Dr. Roberto Peltrini

TUTOR
Prof. Francesco Corcione

ANNO ACCADEMICO 2022/2023

SUMMARY

ABSTRACT

As the uniformity of the brightness in indocyanine green-based fluorescence (ICG) at the time of the anastomosis construction consists only in a qualitative, empirical evaluation, a machine learning algorithm to automatically assess blood perfusion of the bowel stump using NIR-ICG angiography was proposed. Afterwards, the implementation of the algorithm provided the intraoperative identification of the optimal transection line.

The algorithm adopts a *Feed Forward Neural Network* receiving as input a feature vector based on the histogram of the green band of the input image. In particular, the algorithm provides an output that classifies the perfusion as adequate or inadequate. It was used to acquire information related to perfusion during laparoscopic colorectal surgery and suggested the section point based on the ICG intensity, supporting surgeons in assessing objectively the procedure. The algorithm was validated on videos captured during surgical procedures carried out at the University Hospital Federico II in Naples. The results show a classification accuracy of 99.9%, with repeatability of 1.9%. Finally, the real-time operation of the proposed algorithm was tested by analysing the video streaming captured directly from an endoscope available in the operating room.

BACKGROUND

Colorectal Surgery and Anastomotic Leakage

Colorectal carcinoma is the third most common cancer for both men and women and the second leading cause of cancer-related deaths [1]. Although multidisciplinary management of colorectal cancer is the standard of care, surgery remains the cornerstone of the curative treatment. The frequency of sphincter-saving operations for rectal cancer increased from 14% in 1988 to 77% in 2009 [2]. Because of the recent developments in anastomotic stapling devices or popularization of intersphincteric resection (ISR), anastomosis after resection of the rectum has become possible even if the cancer is located close to the anal verge. However, anastomotic leakage (AL) is the most feared complication after colorectal resection because it is associated with increased mortality, reoperation, and definitive stoma formation [3,4].

AL is defined by the International Study Group of Rectal cancer as a defect at the level of the anastomotic site that allows communication between the intraluminal and extraluminal compartments identified through clinical evaluation with digital rectal exploration, endoscopic examination, computed tomography radiological evidence of contrast leakage through the suture gap or the presence of perianastomotic hydro-aerial collection. It is also classified as grade A if it does not affect the postoperative course, grade B when conservative management antibiotic therapy or percutaneous/transanal drainage is required, and grace C when surgical revision is required [5].

AL rates range between 3% and 21% after rectal surgery [5,6], with significant consequences on clinical and economic burden [7].

The negative impact of AL on long-term oncological and functional outcomes has also been demonstrated. In several studies, the risk of local recurrence after rectal cancer surgery was increased in patients with AL [8-10]. Similarly, AL following anterior resection was, in terms of defecatory function, found to increase the risk of aid use to fecal incontinence, whereas defecation frequency trended at being increased. Furthermore, sexual activity was reduced in patients with AL, and the risk of dyspareunia in women trended at being increased [11].

Risk factors for AL include patient-related and technical factors. The former includes male sex, obesity, malnutrition, tobacco use and preoperative radiation and obesity. Although most of these factors are not modifiable at the time of surgery, surgery-related factors can be modified to decrease the risks of AL.

The theoretical concepts to avoid anastomotic complications are well known and based on reducing tension at the anastomotic point and assuring a well perfused proximal colonic stump. Vascular perfusion to the anastomotic region is assessed by the surgeon intraoperatively by various parameters, such as active bleeding from the resection margin, palpable pulsation of the mesentery, and discoloration [12]. However, these methods are considered subjective and highly unreliable [13].

Intraoperative Near-infrared Fluorescence Angiography with Indocyanine Green

Indocyanine green (ICG) is a molecule developed in the 1950s at Kodak's R&D laboratories [14], applied in the field of infrared photography. This molecule is the first substance discovered capable of emitting fluorescence in the near infrared (NIR)

spectrum, as it becomes fluorescent when illuminated with infrared light. This substance has negligible toxicity and is quickly disposed of by the body without side effects, except for rare allergic reactions easy to prevent [15]. In 1959, the Food and Drug Administration (FDA) approved its use in clinical settings, and since then, it has been widely used for diagnostic investigations for pathology affecting heart, eyes, liver, and lungs. In this setting, laser fluorescence using indocyanine green (ICG) dye is a promising and widespread real-time technology because of its easy accessibility, accuracy and cost effectiveness.

Various risk factors are associated with AL, but insufficient blood perfusion is generally considered as one of the main causes [16,17]. ICG is a water soluble, tricarbocyanine dye that provides real-time visualization of vascular structures by emitting fluorescence when stimulated by polarized light [18]. The evaluation of perfusion of the supposed proximal section line starts within 60 s of an intravenous bolus injection of ICG. An NIR camera detects the fluorescence of the microcirculation of the colonic wall receiving adequate vascularization. Therefore, ICG fluorescence reflects the colonic stump perfusion allowing the choice of the most appropriate site for the final section and then for the anastomosis (Figure 1). A second check can be also performed after the anastomosis construction both by injecting a second bolus of ICG to verify fluorescence of the stumps and by transanal endoscopic suture line visualization.

The concept of ICG intraoperative angiography is based on the ability of ICG to absorb near-infrared light (NIR) at 800 nm and to emit fluorescence at a wavelength of 830

nm. Albumin is the most important intravascular binding-protein for ICG so that tissue microperfusion is revealed by the presence of fluorescence. In brief, a bolus of ICG is injected into the patient intravenously, NIR light is then absorbed by ICG in the tissue, and the resulting fluorescence reflects perfusion. A deficiency of perfusion at the anastomotic site increases the risk of dehiscence, which consists in a failure to heal the sutures with the consequent appearance of fistulas and tissue perfusion. The evaluation of the intensity and the uniformity of this fluorescence allows to assert if the parts are adequately perfused. Therefore, assessing the quality of perfusion using ICG allows the surgeon to intervene promptly during surgery.

Jafari et al. [19] assessed the utility of ICG FA in left colectomy and anterior resection in the PILLAR II study. The incidence of AL in their study was 1.4%, with a change in the surgical strategy in 8% of patients. Boni et al. [20] reported that ICG FA could be safely and effectively performed in rectal surgery. The use of IGC-FA changed the surgical plan in 4.7% of their patients and AL did not occur in the ICG group, compared with an incidence of 5.2% in the control group. However, the differences were not statistically significant. The studies agree on the safety and feasibility of the technique and demonstrate its usefulness in the assessment of tissue perfusion.

Several comparative retrospective and prospective studies investigated the relationship between the use of ICG and the 30-d AL rate as the primary outcome [18,21-24]. They showed a statistically significant correlation between ICG FA and reduction in the risk of AL associated with the modification of the proximal section line.

Initially, only three randomized controlled trials (RCTs) addressed the topic. In the first multicentre trial [25], differences in AL or reoperation rates between ICG and the control group (5% *vs* 9% and 6.7% *vs* 6.5%) were not significant. Although the authors confirmed the efficacy of ICG in bowel viability assessment during left colectomy or anterior resection, a real advantage related to AL was not demonstrated and the study suffers from insufficient power due to the small sample size. The FLAG trial [26] involved 377 patients with either malignant or benign sigmoid or rectal neoplasms, 187 in the ICG FA group and 190 in the control group. The results showed that changes in the transection line were performed in almost 20% of patients. A decrease in AL was achieved using ICG FA, but the difference was statistically significant only in cases with low rectal anastomosis (14.4% with ICG FA *vs* 25.7% without ICG FA; $P = 0.04$). The PILLAR III trial planned as a phase III trial for low anterior resection (planned sample size: n= 800 patients), discontinued enrolment in 347 cases and thus was also underpowered [27].

Two recent meta-analyses assessed the role of ICG FA imaging on the incidence of AL after rectal cancer surgery [28,29]. In a pooled analysis of 2088 patients, the AL rate in the ICG group was significantly lower than that in the control group, and the intraoperative use of ICG was associated with a decreased overall complication rate and reduced reoperation rate. However, both analyses suffer from the same limitations as the studies taken into consideration and the lack of RCTs in the analysis.

Recently, the EssentiAL trial [30] involving 850 rectal cancer patients who underwent minimally invasive sphincter-preserving surgery demonstrated that ICG significantly

reduced the anastomotic leakage rate by 4.2%. This is the only trial including exclusively cases of rectal cancer with tumor localization 12 cm or lesser from the anal verge and registered the largest number of patients thus far.

The use of ICG- fluorescence imaging is not a completely standardized technique as there are variables related to the dose of injected ICG (0.013-0.89 mg/kg), the proximity of the laparoscope to the colic wall, the number and type of checks performed, and differences in the equipment available on the market.

Currently, one of the most relevant limitations of the technique is related to its being a subjective evaluation by the surgeon of the intensity of the emitted infrared light. Indeed, there are no systems or techniques used to quantify it, and to objectively support the surgeons in their assessment. At the state of the art, several attempts to design systems capable to help the surgeons in the assessment of perfusion quality have been made [31-34]. These approaches are mostly based on the diffusion speed of the indocyanine in the tissues. The perfusion of the colorectal segment is estimated by looking at the gradient of the intensity of ICG fluorescence brightness captured by the camera. The output provided by these systems is a heat map highlighting the intestinal portions characterized by a faster increase of ICG fluorescence brightness after the injection. Furthermore, they try to correlate the heat map with the post-surgery result. However, the methods described in these works are not able to automatically assess if the perfusion is good or not in the analysed area, as they only provide a graphical output that must be interpreted by the surgeons subjectively.

Artificial Intelligence in Medicine

Artificial Intelligence (AI) is broadly defined as a machine or computing platform that can make intelligent decisions. Two types of AI have generally been pursued in health care delivery: machine learning (ML), which involves computational techniques that learn from examples instead of operating from predefined rules, and natural language processing, which is the ability of a computer to transform human language and unstructured text into machine-readable structured data that reliably reflect the intent of the language [35].

In health care delivery, the role of AI in improving clinical judgment has garnered the most attention, with a particular focus on prognosis, diagnosis, treatment, clinician workflow, and expansion of clinical expertise. Specifically, ML software is based on mathematical algorithms that simulate inductive reasoning, learning from information. This happens through the recognition of patterns, that is of the regularities in the data that allow to classify determined situations and to lead them back to specific outcomes. In this way, predictive models are generated which make it possible to understand that certain combinations of values of certain parameters are often associated with specific outputs [36].

Based on the learning paradigm there are three types of machine learning:

• Supervised Learning. It is the most widely used. Just as a child learns to identify fruits by memorizing them in an illustrated book, in machine learning supervised the algorithm learns from a data set already labelled and with a predefined output.

• Unsupervised Learning. It uses a more independent approach, in which a computer learns to identify complex processes and patterns without the guidance of the programmer. Unsupervised machine learning involves data-based training without labels and for which no specific output has been defined.

• Reinforcement Learning. In this case learning is based on feedback. Unlike the other two, this paradigm addresses problems of sequential decisions, in which the action to be taken depends on the current state of the system and determines the future one. The quality of an action is given by a score which aims to encourage choices with higher scores.

There are many examples of ML-based approaches used in colorectal surgery, as proof that this technology can help and assist surgeons to minimize the risks for the patients and prevent complications. A decision support system based on AI was used by Cahill et al. [37] in colorectal cancer intra-operative tissue classification. Instead, Park et al. [38] adopted AI to evaluate the feasibility of AI-based real-time analysis of microperfusion to predict the risk of anastomotic complication in the patient with laparoscopic colorectal cancer surgery. The first study showing the useful of an image-guided navigation system with total mesorectal excision was conducted by Igaki et al. [39]. Furthermore, AI was used to improve colorectal polyps detection during colonoscopy [40] and to identify laparoscopic surgical videos, in order to facilitate the automation of time-consuming manual processes, such as video analysis, indexing, and video-based skill assessment [41]. Nevertheless, there are still no methods based on AI that automatically assess the quality of perfusion in the analysed area.

INTRODUCTION

The research project was carried out in two phases. First, the proposal was a ML-based real-time system to objectively assess the adequate perfusion of the colonic stump after an injection of ICG. This system is used to acquire information related to perfusion during laparoscopic colorectal surgery and objectively support the surgeon during anastomosis construction. In particular, the algorithm provides an output that classifies the perfusion as *adequate* or *inadequate*. Second, developing the algorithm to provide the optimal transection line during colorectal resections to perform a safe anastomosis.

PHASE 1: QUALITY OF PERFUSION ASSESSMENT

Architecture of the Neural Network

The problem addressed in this work can be formally expressed as a two-class classification problem involving frames (from a video streaming) corresponding to an adequately - or inadequately - perfused area. The system works on a video extracted from a laparoscopic camera and a Region of Interest (ROI). The ROI is selected by a member of the operating room team (e.g., an assistant surgeon) and contains the area to be assessed. To this purpose, the idea was to develop a system that automatically assesses the quantity of ICG present in the ROI, by computing the histogram of the green band of the acquired frames, then providing an output corresponding to an *adequate* or to an *inadequate* perfusion.

The overall architecture of the proposed system is shown in Fig. 1. The input of the system are (i) the frames coming from the *Video streaming*, and (ii) the *ROI* identified as a rectangular box selected by the user. The ROI, which identifies the portion of the frame to be analysed, is selected by the OR operator using the mouse or the track-pad on the computer when starting the algorithm. The architecture, from left to right, is composed of the following three functional blocks:

• The first block consists of a *Fast tracking algorithm*, which is used to track the selected ROI during the video execution. In particular, the Minimum Output Sum of Squared Error (MOSSE) tracker33 was exploited, as it uses adaptive correlation to track objects, resulting in a better robustness to variations in lightning, pose, scale and non-rigid transformations. The MOSSE implements also an auto pause and resume

functionality if the object to track disappears (for example, if the surgeon covers it) and then it reappears again. Moreover, the exploited tracker can work at high frame rates (more than 450 fps).

• Once the frames containing the ROI are extracted from the video source, the second block performs a *Features extraction*. The frames are in the RGB format, namely the colored image is obtained by a combination of three images, one for each color channel: red, green and blue. Each pixel has an 8-bit resolution; this value represents the intensity of the pixel. Afterwards, the ROI of each frame is divided into 20 vertical equal slices and, for each of them, the histogram of the green band and its area is computed. Finally, a vector of 20 elements (*features vector*) is obtained. This vector becomes the input to the last functional block.

• This step of the process binarily *Classifies* the feature vector and establishes whether it corresponds to an *adequate/1* or to a *inadequate/0* perfusion of the colorectal portion. This classifier is obtained by a Feed Forward Neural Network (FFNN).

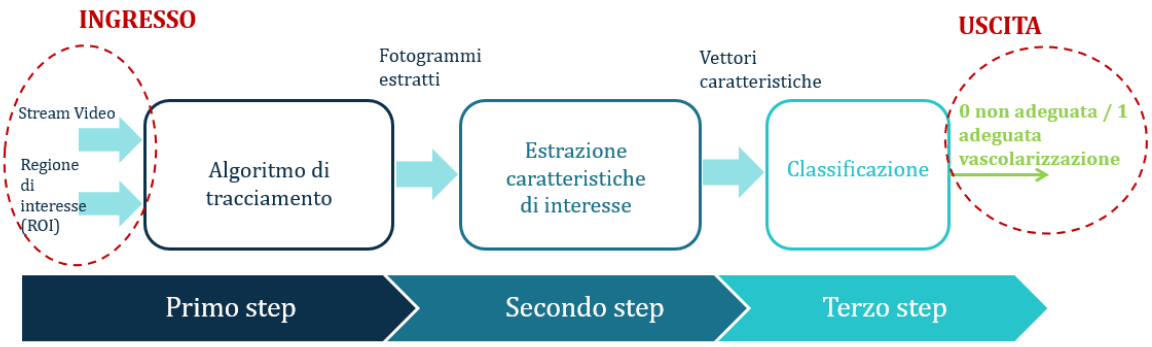

Figure 1. Block architecture of the proposed algorithm. Three main blocks are outlined: (i) a fast-tracking algorithm to track the selected ROI, (ii) a feature extraction block to pre-process the available frames and (iii) a ML-based classifier to provide the output in terms of quality of perfusion.

Model evaluation and selection

The following Neural Networks (NN) were evaluated as classifiers:

• *One-hidden-layer NN*: In this case, a classic feed forward neural network (FFNN) with one hidden layer was used. The output layer had a single neuron with a sigmoidal activation function. The hidden layer was preliminary tested with (i) 20 neurons and a *Rectifier Linear Unit* (ReLU) activation function, and (ii) 80 neurons and a *Tanh* activation function. After, this network was further tested with the following activation functions: *Tanh*, *Sigmoid*, and *Rectifier Linear Unit* (ReLU): here, for each activation function the number of neurons changed between 10 and 100, with step 10.

• *Two-hidden-layer NN*: In this case, a FFNN composed by 2 hidden layers was used. Different combinations of *ReLU*, *Sigmoid* and *Tanh* activation function, considering a number of neurons equal to 50, 70, and 90, were tested. *SoftMax* activation function, and two neurons were used for the output layer.

Operative details

Patients who underwent to elective laparoscopic or robotic left colectomy or anterior rectal resection with primary anastomosis were included. Standard resection with complete mobilization of the splenic flexure and tumor-specific mesorectal excision for rectal cancer. The specimen was extracted through a suprapubic incision. After dividing the mesentery and the marginal vessels at a point appropriate for the proximal margin, a dose of 0.25 mg/Kg of ICG is administered intravenously by bolus injection followed by a saline flush (10 mL). An 18-gauge peripheral catheter in the forearm is

used for injection. The blood flow in the proximal colon is evaluated by using a NIR camera system: Olympus CH-S200 camera with 30°, 10-mm IR telescope for laparoscopic surgery. The camera is fixed 15 cm apart from the extracted specimen and lights of the operating room are completely turned off. The imaging data are recorded starting before ICG injection and for more than n minutes after injection is completed. This moment is indicated by a thumbs up on the video. Continuous monitoring of systemic perfusion factors during surgery is performed to ensure their stability during fluorescence evaluation. Cardiac Index (CI), Systemic Vascular Resistance Index (SVRI) and Mean Arterial Pressure (MAP) are monitored by using the EV1000 clinical platform (Edwards Lifesciences Corporation). The following values should be pursued: CI 2.8-3.2 L/min/m 2, SVRI 1800-2100 dynes · sec/cm5/m2, MAP > 60 and < 90 mmHg.

Preclinical setup

A total of 11 videos in .M4V format were provided by the surgeons: the videos were collected and labelled by the medical staff during routine clinical practice. An anonymisation procedure was applied to protect patients' privacy. Specifically, any metadata was removed from the original files. These files contain the video, acquired directly from the endoscope during surgery, related to the portions of the intestine where the anastomosis was being performed. When the ICG was injected, the portion that was well perfused became fluorescent. An example of frames extracted from the dataset is shown in Fig. 2, which shows the intraoperative use of ICG technology.

Specifically, Fig. 2a refers to the fluorescence angiography which shows the vascular perfusion of the intestinal segment that delimits the section point. Fig. 2b shows the anastomosis being performed with the residual colon. Fluorescence angiography was performed using a laparoscopic system (*Olympus OTV-S300*, Olympus Europe SE & Co. KG, Hamburg, Germany) with a light source (*Olympus CLV-S200 IR*) which allowed the use of both visible and near-infrared light.

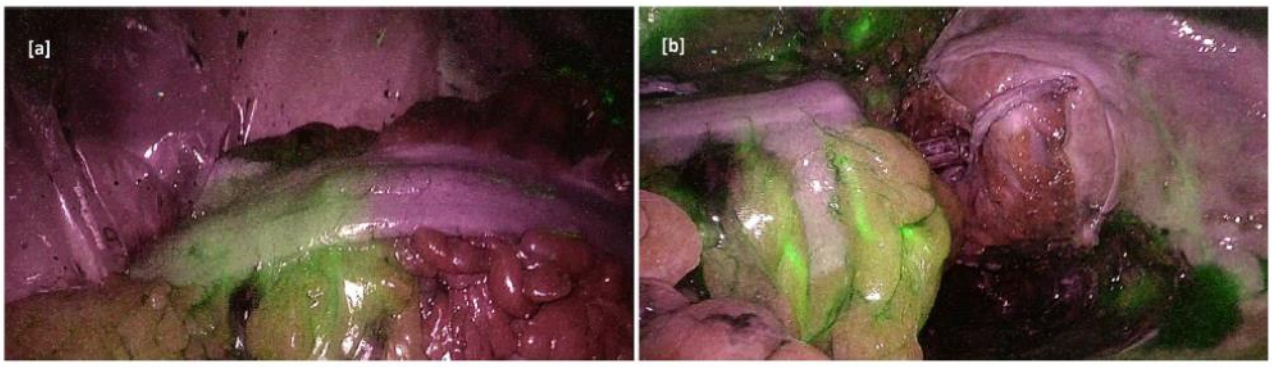

Figure 2. Intraoperative use of ICG technology. Fluorescence angiography shows the vascular perfusion of the intestinal segment that delimits the section point (**a**). Anastomosis is performed with the residual colon (**b**).

The performance of the developed NNs was validated by processing the 11 videos available from the dataset. From each video of the data set, different frames were extracted. To properly train the model in assessing the quality of perfusion, frames containing ROIs with clear evidence of ICG were selected as well as more tricky ones. From each ROI, 20 features vectors were obtained. The total size of the dataset is constituted by 470 frames. Figure 3 illustrates the overall process of features extraction. The considered frame is shown in Step 1. As aforementioned, the ROI selected by the user is splitted into 20 slices (Step 2); therefore, for each obtained slice (Step 3), the

histogram of green, showing the occurrence of each level of green, is computed (Step 4). The area of the histogram constitutes an element of the feature vector.

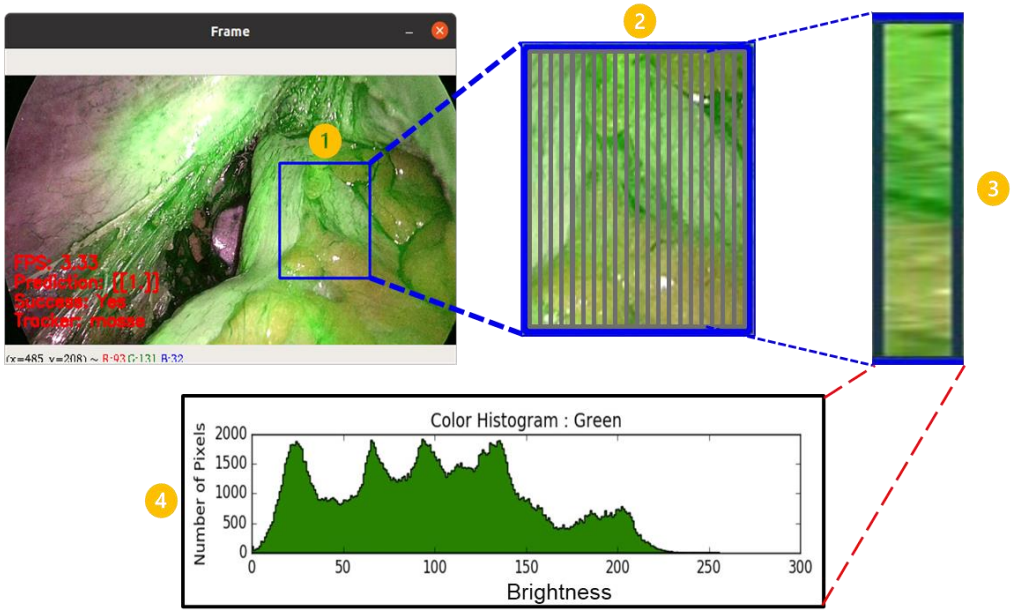

Figure 3. Details about the features extraction: Step 1: selection of the ROI. Step 2: the ROI is divided in 20 slices. Step 3: for each slice, the histogram of the green band is evaluated. Step 4: the amount of green of each histogram is evaluated and the obtained feature is used to build the feature vector sent to the ML classifier.

The extracted features are given as input to the aforementioned Classifiers: in Table 1 the chosen set of hyper parameters for each of the classifiers with the corresponding obtained accuracy, in terms of means and 1 −sigma repeatability, is summarized. The obtained experimental results show that the one-hidden layer (L1) NN with 20 neurons and ReLU as activation function is the one that achieves the best performance, with an average accuracy of 99.9% and a 1 − sigma repeatability of 1.9%. Since the NN with one hidden layer achieved the best results, further tests were dedicated to fine tune the number of neurons.

Network	Kernel	Neurons L1	Neurons L2	Activation function	Accuracy (%)
SVM	Linear	–	–	–	54.5 ± 15.6
SVM	Gaussian	–	–	–	45.4 ± 23.8
FFNN	–	20	–	ReLU	99.9 ± 1.9
FFNN	–	80	–	Tanh	54.1 ± 28.6
FFNN	–	100	–	Sigmoid	86.0 ± 7.6
FFNN	–	90	90	ReLU	85.2 ± 15.0
FFNN	–	50	50	Tanh	69.9 ± 22.9
FFNN	–	90	70	Sigmoid	68.5 ± 24.2

Table 1. Performance with the chosen set of hyper parameters for all the tested networks.

Table 2 summarizes the detail of the performance for the one-hidden layer networks as both the number of neurons and the activation function are varied. It can be observed that the best results are always obtained using ReLU as activation function. The number of neurons which achieved the greatest accuracy was confirmed to be 20.

Neurons	Tanh accuracy (%)	Sigmoid accuracy (%)	ReLU accuracy (%)
10	47.9 ± 23.7	74.2 ± 10.6	93.7 ± 14.8
20	42.1 ± 25.3	75.6 ± 14.7	99.9 ± 1.9
30	51.1 ± 28.1	79.5 ± 11.5	98.0 ± 3.0
40	45.6 ± 39.5	79.4 ± 8.5	97.4 ± 5.2
50	53.2 ± 36.1	84.6 ± 9.2	97.4 ± 3.2
60	52.1 ± 35.9	85.8 ± 5.5	98.6 ± 2.8
70	49.1 ± 33.2	81.1 ± 10.7	99.3 ± 2.0
80	54.1 ± 28.6	83.7 ± 9.8	99.4 ± 1.9
90	50.9 ± 34.2	82.6 ± 6.4	98.7 ± 2.7
100	53.9 ± 30.2	86.0 ± 7.6	99.7 ± 2.6

Table 2. Performance of FFNN with one hidden layer and Tanh, Sigmoid, and ReLU as activation functions with different neurons.

Statistical analysis

The results reported in Table 2 were statistically validated by means of One-Way *ANOVA* and *Fischer test*, by verifying the statistical significance of the differences between the mean accuracies obtained by the three different activation functions used (Tanh, Sigmoid, and ReLU). The chosen null hypothesis H0 was that the groups belonged to the same population with a significance level alfa = 1.0%. The test rejected the null hypothesis with a *P*-value = 0.0%. Therefore, the *Paired t-test* was carried out to understand which of the three groups is different from the others. The significance level alfa was again set equal to 1.0%. For all three tests the hypothesis H0, that assumed the groups were identical, was rejected. The analysis was conducted by means of the online tool *Statistic Kindgom*40. Further details are reported in Table 3.

The tests confirmed that the results obtained with ReLU activation function and 20 neurons are statistically relevant. In fact, there is a significant difference between this model and the others with different activation functions. Hence, this model was chosen for the classification stage of the proposed system and used in the prototype version.

Test	H_0	α (%)	*P*-value (%)	Decision
Fischer test Tanh-Sigmoid-ReLU	Same distribution	1.0	0.0	Reject
t-test Tanh-Sigmoid	Same distribution	1.0	$1.8 \cdot 10^{-9}$	Reject
t-test Tanh-ReLU	Same distribution	1.0	$3.5 \cdot 10^{-9}$	Reject
t-test ReLU-Sigmoid	Same distribution	1.0	$1.0 \cdot 10^{-5}$	Reject

Table 3. Details about statistical analysis of the three groups.

Preclinical Results

Figure 4 shows the results obtained by applying the proposed algorithm to frames of the data set with good and bad perfusion. For each considered frame, the corresponding ROI is indicated. In particular, Fig. 4a and d have ROI classified with good perfusion (good amount of green) and prediction 1. On the other hand, Fig. 4b and c has prediction output equal to 0 because the ROI are considered by the algorithm as bad perfused due to a low grade of green or due to a not uniform presence of green in the selected ROI. In each of the considered cases, the correctness of the classification was confirmed by the surgeons.

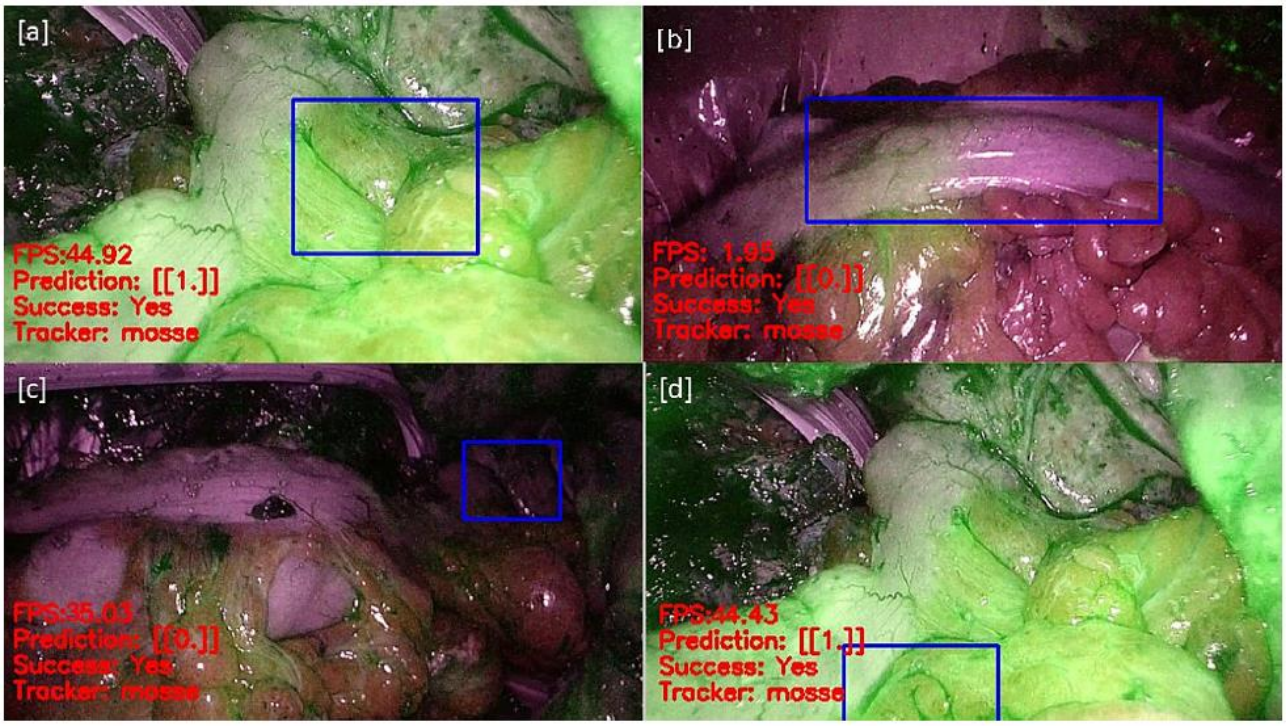

Figure 4. Four frames from the data set with respective ROI: (**a**) and (**d**) have ROI with adequate perfusion (high amount of green) and prediction 1. (**b**) and (**c**) have prediction 0 because the ROIs are inadequately perfused (low amount of green and/or not uniform ICG diffusion).

Intraoperative experimental validation

After the offline validation, the algorithm was further validated using the equipment available at the University Hospital *Federico II* in Naples, Italy. The aim was to ensure the possibility of interfacing the proposed system with the medical equipment. An additional aspect to consider is, in fact, the real-time interfacing with the endoscope. The endoscope used was the *Olympus Visera Elite II*. It is an imaging platform for general surgery, urology, gynecology, and more, which links the OR to other devices and facilities around the hospital. An S-video to USB adapter was used to connect the endoscope to a PC equipped with Windows 10 and Python 2.7.

The video captured from the endoscope was transmitted in real time to an elaboration unit kept outside the OR. Therefore, surgeons who did not take part in the operation were asked to select the ROIs. However, this workflow can be also conducted by the main surgical team inside the OR.

The algorithm was able to receive and process at least 30 frame per seconds (fps) from the video source: this frame rate was considered acceptable for the surgeons to select the ROI and use the system. Moreover, the output provided by the algorithm might effectively help surgeons to take the decision even in unclear situations (i.e., low brightness).

These additional trials demonstrated the feasibility of the practical implementation of the proposed MLbased algorithm Fig. 5, the output of the system working under three different levels of green brightness is shown. This also demonstrates that the proposed system is able to correctly classify the frame regardless of the level of green brightness.

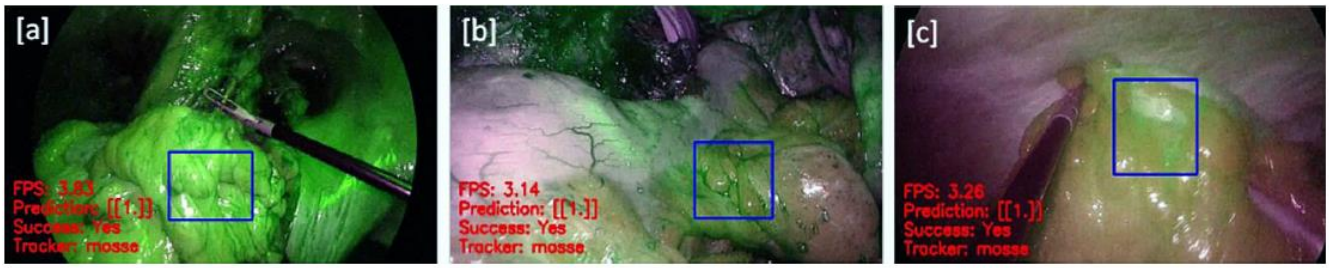

Figure 5. Online validation: Frames characterized by different brightness levels acquired directly from the endoscope during the online validation: (**a**) is characterized by high brightness, (**b**) by medium brightness, and (**c**) by low brightness. Nevertheless, the real-time prediction works even in a low brightness scenario.

PHASE 2: PREDICTION OF THE TRANSECTION LINE

Architecture of the Neural Network

In the previous steps a matrix of 20 columns is built, one for each slice, whose rows represent the number of processed frames. The resulting matrix indicates the green change over time and represents the input of a neural network. The network associates a probability to each slice, to the maximum value corresponds to the final prediction. The prediction is displayed on the video as a red line at the chosen slice (Fig. 6). The transection line is predicted in real time so it can change whenever the video changes. A message is displayed when the prediction reaches the convergence value.

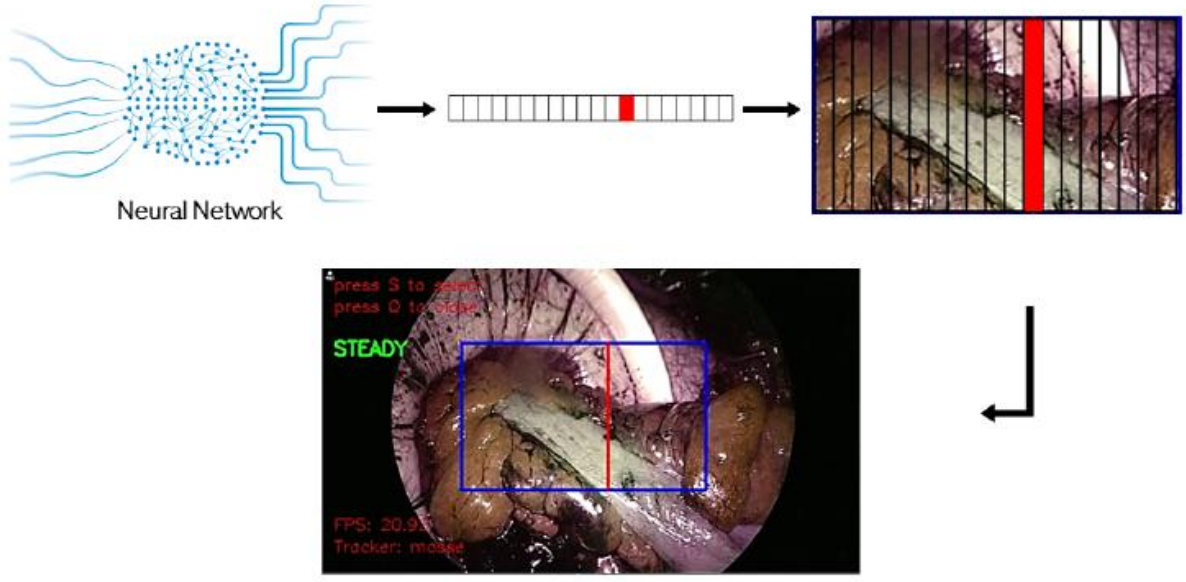

Figure 6. The final algorithm steps.

The problem addressed in this case can be formally expressed as a twenty-class classification problem. The network used is composed of 2 hidden layers and the output

layer with Softmax activation function. A 200 neuronal network with sigmoid activation function achieved the best accuracy (Fig.7).

Figure 7. Network performance evaluation by varying the neurons number of the first layer considering two sigmoids as activation function.

Intraoperative experimental validation

The first step is to acquire the video, it can be a video loaded on the PC or it can be acquired from the webcam or endoscope. Once the acquisition source has been defined, the operator will see an image similar to the one in Figure 8. In the top left corner, there is a red writing urging selection, which can be done by pressing the S key. At this point, the operator can use the mouse to draw a blue rectangle surrounding the stretch of colon that is to be severed.

Figure 8. Video capture

To confirm the selection, a new text string appears, prompting you to press the Enter key, as shown in Figure 10. Instantly the tracker starts tracking the region marked by the rectangle and the prediction of the network corresponding to a red segment is shown on the screen. The frame rate value obtained differs depending on the acquisition mode. Acquiring video from a computer is in the range of 10fps to 30fps, while acquiring from a webcam or external source (such as an endoscope) increases between 40fps and 100fps.

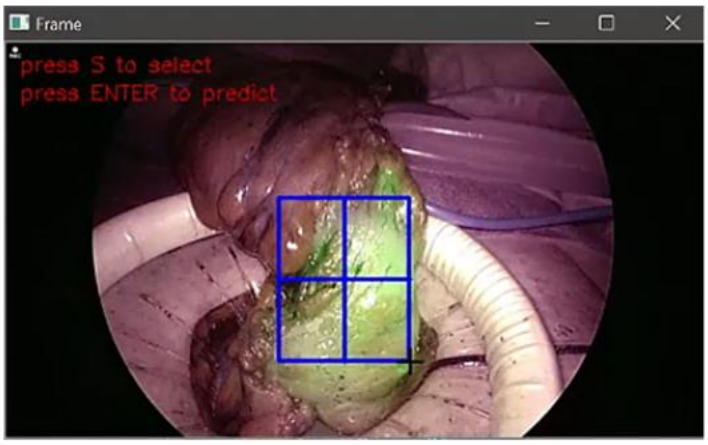

Figure 9. Confirm the selection and start ROI tracking

The current values of the frame rate and the tracker object used by the program are shown in Figure 10. The prediction continues to be visible and after about 10 seconds during which it has not changed, the steady message appears, which ensures the convergence of the predictions. To close the execution of the program, press the Q key as shown in the instructions on the screen in Ultimately, the goodness of the network prediction is shown.

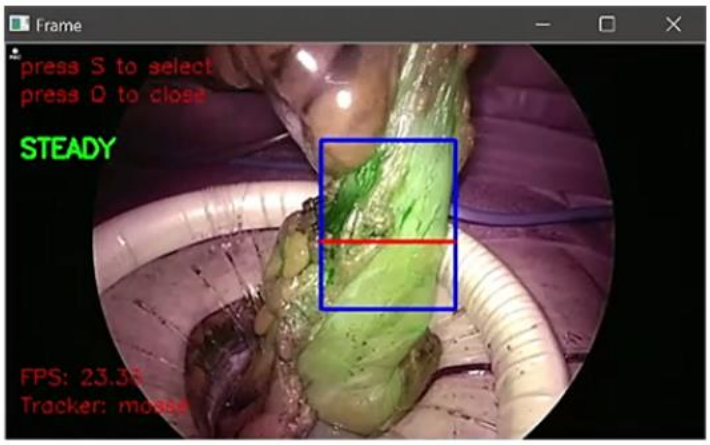

Figure 10. Steady state of network predictions

In Figure 11 is clear how the predicted transection line corresponds perfectly to the one decided to the medical team.

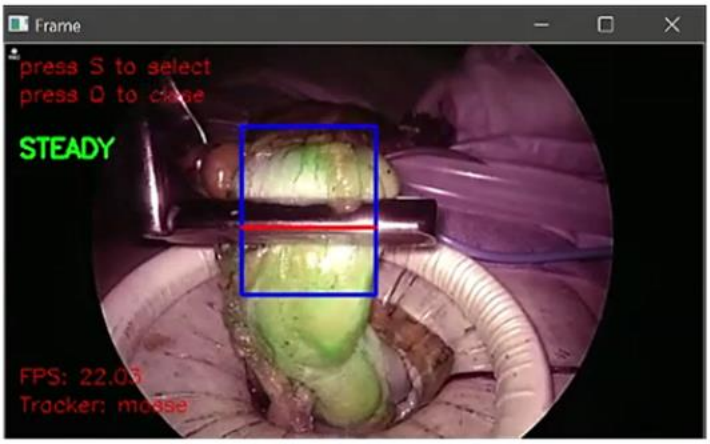

Figure 11. The predicted transection line corresponds perfectly to the one decided to the medical team.

LIMITATIONS AND FUTURE PERSPECTIVES

The system suffers from a small dataset. Therefore, it would be better increase input data to train the network. In addition, a correlation between intraoperative setting and postoperative period should be conducted to provide a clinical efficacy.

Future work will be addressed to overcome the current research weakness, by (i) introducing more levels between adequate and inadequate perfusion, in order to increase the resolution of the assessment and further enhance accuracy of prediction, (ii) identifying a method to automatically select the ROIs, and (iii) enrich the dataset by facing circumstances when the blood perfusion is impaired by underlying pathologies (e.g., atherosclerosis). In this case, in fact, both the classifier and the surgeon are not trained to correctly assess whether perfusion is adequate or not.

Finally, as the ICG images are also affected by the NIR illumination intensity, camera exposure time, shooting distance and other parameters, the algorithm was further improved by integrating various analysis factors. Specifically, ICG intensity/time pattern curves will be assessed to provide a more accurate real-time analysis of the perfusion during surgery.

CONCLUSIONS

A system based on ML classifiers is proposed to assist the surgeons during laparoscopic colorectal surgery. It is a decision-support system able to automatically assess if the quality of the perfusion is *adequate* or *inadequate* after an injection of indiocyainine green dye. Different models of classifiers were tested on a dataset of videos of several anastomoses carried out at the Federico II Hospital. Overall, the one-hidden-layer NN with 20 neurons and ReLU activation function achieved the best performance. In fact, the obtained results showed a prediction accuracy of 99.9% with a $1 -$ repeatability of 1.9%. These results were statistically validated by means of (i) ANOVA, and (ii) Fischer and Paired-t tests. Therefore, this model was selected for the system implementation. The proposed system was successfully validated also in relation to the interfacing with actual equipment used at the University Hospital *Federico II* in Naples, Italy. It can represent an important decision support to surgeons during the operation, especially in condition of uncertainty - where it is not clear whether the blood perfusion is adequate or not - due to an unclear presence of ICG. Furthermore, the algorithm can provide a decision support tool to the surgeon on the assessment of the transection line. This real-time analysis may improve the intraoperative use of the ICG fluorescence angiography with an objective prediction of the resection line.

REFERENCES

[1] Siegel RL, Miller KD, Jemal A. Cancer statistics, 2020. CA Cancer J Clin 2020; 70: 7-30.

[2] Gerard JP, Rostom Y, Gal J, et al. Can we increase the chance of sphincter saving surgery in rectal cancer with neoadjuvant treatments: lessons from a systematic review of recent randomized trials. Crit Rev Oncol Hematol. 2012;81:21–28.

[3] Peeters KC, Tollenaar RA, Marijnen CA, Klein Kranenbarg E, Steup WH, Wiggers T, Rutten HJ, van de Velde CJ; Dutch Colorectal Cancer Group. Risk factors for anastomotic failure after total mesorectal excision of rectal cancer. Br J Surg 2005; 92: 211-216

[4] Matthiessen P, Hallböök O, Andersson M, Rutegård J, Sjödahl R. Risk factors for anastomotic leakage after anterior resection of the rectum. Colorectal Dis 2004; 6: 462-469

[5] Rahbari NN, Weitz J, Hohenberger W, Heald RJ, Moran B, Ulrich A, et al. Definition and grading of anastomotic leakage following anterior resection of the rectum: a proposal by the International Study Group of Rectal Cancer. Surgery. (2010) 147:339–51.

[6] Degiuli M, Elmore U, De Luca R, De Nardi P, Tomatis M, Biondi A, et al. Risk factors for anastomotic leakage after anterior resection for rectal cancer (RALAR study): a nationwide retrospective study of the Italian Society of Surgical Oncology Colorectal Cancer Network Collaborative Group. Colorectal Dis. (2022) 24:264–76.

[7] Hammond J, Lim S, Wan Y, Gao X, Patkar A. The burden of gastrointestinal anastomotic leaks: an evaluation of clinical and economic outcomes. J Gastrointest Surg. (2014) 18:1176–85.

[8] Hain E, Maggiori L, Manceau G, Mongin C, Prost À la Denise J, Panis Y. Oncological impact of anastomotic leakage after laparoscopic mesorectal excision. Br J Surg. 2017 Feb;104(3):288-295.

[9] Peltrini R, Carannante F, Costa G, Bianco G, Garbarino GM, Canali G, Mercantini P, Bracale U, Corcione F, Caricato M, Capolupo GT. Oncological outcomes of rectal cancer patients with anastomotic leakage: A multicenter case-control study. Front Surg. 2022 Sep 12;9:993650.

[10] Koedam T, Bootsma BT, Deijen CL, van de Brug T, Kazemier G, Cuesta MA, et al. Oncological outcomes after anastomotic leakage after surgery for colon or rectal cancer: increased risk of local recurrence. Ann Surg. (2022) 275:e420–7.

[11] Kverneng Hultberg D, Svensson J, Jutesten H, Rutegård J, Matthiessen P, Lydrup ML, Rutegård M. The Impact of Anastomotic Leakage on Long-term Function After Anterior Resection for Rectal Cancer. Dis Colon Rectum. 2020 May;63(5):619-628.

[12] Kudszus S, Roesel C, Schachtrupp A, et al. Intraoperative laser fluorescence angiography in colorectal surgery: a noninvasive analysis to reduce the rate of anastomotic leakage. Langenbecks Arch Surg 2010; 395(8):1025-1030.

[13] Karliczek A, Harlaar NJ, Zeebregts CJ, et al. Surgeons lack predictive accuracy for anastomotic leakage in gastrointestinal surgery. Int J Colorectal Dis 2009; 24(5):569-576.

[14] Donnachie, E. M. et al. Indocyanine green interference in the Kodak Ektachem determination of total bilirubin. Clin. Chem. **35**, 899–900.

[15] Benya, R., Quintana, J. & Brundage, B. Adverse reactions to indocyanine green: a case report and a review of the literature. Cathet. Cardiovasc. Diagn. **17**, 231–233 (1989).

[16] Attard JA, Raval MJ, Martin GR, Kolb J, Afrouzian M, Buie WD, Sigalet DL. The effects of systemic hypoxia on colon anastomotic healing: an animal model. Dis Colon Rectum 2005; 48: 1460-1470.

[17] Vignali A, Gianotti L, Braga M, Radaelli G, Malvezzi L, Di Carlo V. Altered microperfusion at the rectal stump is predictive for rectal anastomotic leak. Dis Colon Rectum 2000; 43: 76-82.

[18] Impellizzeri HG, Pulvirenti A, Inama M, Bacchion M, Marrano E, Creciun M, Casaril A, Moretto G. Near-infrared fluorescence angiography for colorectal surgery is associated with a reduction of anastomotic leak rate. Updates Surg 2020; **72**: 991-998.

[19] Jafari MD, Wexner SD, Martz JE, McLemore EC, Margolin DA, Sherwinter DA, Lee SW, Senagore AJ, Phelan MJ, Stamos MJ. Perfusion assessment in laparoscopic left-sided/anterior resection (PILLAR II): a multi-institutional study. J Am Coll Surg 2015; 220: 82-92.e1

[20] Boni L, Fingerhut A, Marzorati A, Rausei S, Dionigi G, Cassinotti E. Indocyanine green fluorescence angiography during laparoscopic low anterior resection: results of a case-matched study. Surg Endosc 2017; **31**: 1836-1840

[21] Losurdo P, Mis TC, Cosola D, Bonadio L, Giudici F, Casagranda B, Bortul M, de Manzini N. Anastomosis Leak: Is There Still a Place for Indocyanine Green

Fluorescence Imaging in Colon- Rectal Surgery? Surg Innov 2020; 1553350620975258.

[22] Hasegawa H, Tsukada Y, Wakabayashi M, Nomura S, Sasaki T, Nishizawa Y, Ikeda K, Akimoto T, Ito M. Impact of intraoperative indocyanine green fluorescence angiography on anastomotic leakage after laparoscopic sphincter-sparing surgery for malignant rectal tumors. Int J Colorectal Dis 2020; 35: 471-480.

[23] Otero-Piñeiro AM, de Lacy FB, Van Laarhoven JJ, Martín-Perez B, Valverde S, Bravo R, Lacy AM. The impact of fluorescence angiography on anastomotic leak rate following transanal total mesorectal excision for rectal cancer: a comparative study. Surg Endosc 2021; 35: 754-762.

[24] Benčurik V, Škrovina M, Martínek L, Bartoš J, Macháčková M, Dosoudil M, Štěpánová E, Přibylová L, Briš R, Vomáčková K. Intraoperative fluorescence angiography and risk factors of anastomotic leakage in mini-invasive low rectal resections. Surg Endosc 2021; 35: 5015-5023.

[25] De Nardi P, Elmore U, Maggi G, Maggiore R, Boni L, Cassinotti E, Fumagalli U, Gardani M, De Pascale S, Parise P, Vignali A, Rosati R. Intraoperative angiography with indocyanine green to assess anastomosis perfusion in patients undergoing laparoscopic colorectal resection: results of a multicenter randomized controlled trial. Surg Endosc 2020; 34: 53-60.

[26] Alekseev M, Rybakov E, Shelygin Y, Chernyshov S, Zarodnyuk I. A study investigating the perfusion of colorectal anastomoses using fluorescence angiography: results of the FLAG randomized trial. Colorectal Dis 2020; 22: 1147-1153.

[27] Jafari MD, Pigazzi A, McLemore EC, et al. Perfusion Assessment in Left-Sided/Low Anterior Resection (PILLAR III): a randomized, controlled, parallel, multicenter study assessing perfusion outcomes with PINPOINT near-infrared fluorescence imaging in low anterior resection. Dis Colon Rectum. 2021;64:995–1002.

[28] Shen Y, Yang T, Yang J, Meng W, Wang Z. Intraoperative indocyanine green fluorescence angiography to prevent anastomotic leak after low anterior resection for rectal cancer: a metaanalysis. *ANZ J Surg* 2020; 90: 2193-2200.

[29] Song M, Liu J, Xia D, Yao H, Tian G, Chen X, Liu Y, Jiang Y, Li Z. Assessment of intraoperative use of indocyanine green fluorescence imaging on the incidence of anastomotic leakage after rectal cancer surgery: a PRISMA-compliant systematic review and meta-analysis. *Tech Coloproctol* 2021; 25: 49-58.

[30] Watanabe J, Takemasa I, Kotake M et al. Blood Perfusion Assessment by Indocyanine Green Fluorescence Imaging for Minimally Invasive Rectal Cancer

Surgery (EssentiAL trial): A Randomized Clinical Trial. Ann Surg. 2023 Oct 1;278(4):e688-e694.

[31] Wada, T. et al. Icg fluorescence imaging for quantitative evaluation of colonic perfusion in laparoscopic colorectal surgery. Surg. Endosc. 31, 4184–4193 (2017).

[32] Zehetner, J. et al. Intraoperative assessment of perfusion of the gastric graft and correlation with anastomotic leaks after esophagectomy. *Ann. Surg.* 262, 74 (2015).

[33] Diana, M. et al. Intraoperative fluorescence-based enhanced reality laparoscopic real-time imaging to assess bowel perfusion at the anastomotic site in an experimental model. BJS 102, e169–e176 (2015).

[34] Lütken, C. D., Achiam, M. P., Svendsen, M. B., Boni, L. & Nerup, N. Optimizing quantitative fluorescence angiography for visceral perfusion assessment. Surg. Endosc. 1–11 (2020).

[35] Sahni NR, Carrus B. Artificial Intelligence in U.S. Health Care Delivery. N Engl J Med. 2023 Jul 27;389(4):348-358.

[36] N. Musacchio, G. Guaita, A. Ozzello, M.A. Pellegrini, P. Ponzani, R. Zilich, A. De Micheli, in " Intelligenza Artificiale e Big Data in ambito medico: prospettive, opportunità, criticità ", Journal of AMD, vol. 21-3, 2018.

[37] Cahill, R. et al. Artificial intelligence indocyanine green (icg) perfusion for colorectal cancer intra-operative tissue classification. *Br. J. Surg.* 108, 5–9 (2021)

[38] Park, S.-H. et al. Artificial intelligence based real-time microcirculation analysis system for laparoscopic colorectal surgery. World J. Gastroenterol. 26, 6945 (2020).

[39] Igaki, T. et al. Artificial intelligence-based total mesorectal excision plane navigation in laparoscopic colorectal surgery. Dis. Colon Rectum 65, e329–e333 (2022).

[40] Sánchez-Peralta, L. F., Bote-Curiel, L., Picón, A., Sánchez-Margallo, F. M. & Pagador, J. B. Deep learning to find colorectal polyps in colonoscopy: A systematic literature review. Artif. Intell. Med. 108, 101923 (2020).

[41] Kitaguchi, D. et al. Automated laparoscopic colorectal surgery workflow recognition using artificial intelligence: Experimental research. Int. J. Surg. 79, 88–94 (2020).